BioNanoScience
https://doi.org/10.1007/s12668-019-00642-y

Comparative Analysis of Toxicity Induced by Different Synthetic Silver Nanoparticles in Albino Mice

Atif Yaqub[1] · Sarwar Allah Ditta[1] · Khalid Mahmood Anjum[2] · Fouzia Tanvir[1] · Naila Malkani[1] · Muhammad Zubair Yousaf[3]

Abstract
Use of nanoparticles for various industrial and biomedical applications has emerged in recent years rapidly, but their accumulation in the environment has raised concerns for their ecotoxicological profile. Instead of halting their use, emphasis should be laid to the development of safer nanoparticles. We prepared silver nanoparticles (AgNPs) by chemical synthesis as well by green synthesis method using *Ocimum tenuiflorum* L. plant. Characterization of green synthesized silver nanoparticles (G. AgNPs) and chemically synthesized silver nanoparticles (C. AgNPs) was performed; UV-visible confirmed the optical absorption peaks at 425 nm (G. AgNPs) and 416 nm (C. AgNPs). SEM imaging confirmed the spherical shaped G. AgNPs (40–60 nm) and C. AgNPs (30–40 nm) with average sizes. FTIR analysis of G. AgNPs confirmed that alkene and aromatic compounds played an important role as capping and reducing agent. We also attempted to evaluate the toxicity profile using a mammalian model, male albino mice (BALB/c)x LD50 of the G. AgNPs and C. AgNPs for mice were found to be 812 mg/kg and 575 mg/kg of the body weight respectively. Liver enzymes were studied from liver tissue and blood serum samples collected from G. AgNP-treated and C. AgNP (100 mg/kg dose)-treated mice for 21 days. We observed a significant decrease in catalase (72.8 versus 86) and GST (0.4 versus 0.32) for G. AgNPs vs C. AgNPs respectively; whereas an increase of SOD is reported (3.05 vs 2.26 respectively). Hence, the development of nanoparticles by green synthesis may be the safer, cost-effective, and eco-friendly option as compared to chemical synthesis.

Keywords Green synthesis · Silver nanoparticles · Acute toxicity · Oxidative stress · Superoxide dismutase · Catalase · Glutathione-S-transferase

1 Introduction

Nanotechnology has emerged as an interesting area of science, because of its wide range applications in the biomedical and health sciences, and regular research is being conducted on the metallic nanomaterials and their potential applications [1, 2]. Development of novel nanomaterials with unique properties, with desired functions and abilities, is necessary for the recent era.

✉ Atif Yaqub
atif@gcu.edu.pk

[1] Department of Zoology, Government College University, Lahore, Pakistan

[2] Department of Wildlife and Ecology, the University of Veterinary and Animal Sciences, Lahore, Pakistan

[3] Department of Biological Sciences, F.C. College University, Lahore, Pakistan

Nanomaterials entry into the environment is damaging and harmful for the living systems, as these materials are deleterious and toxic, so their potential impacts and toxicity profiling are very important and essential to deal with their future impacts on the ecosystem [3]; and along with their risk analyses, safer nanoparticles development is more essential to cope with the need of nanomaterials, which are more secure and safe for the ecological well-being as compared to the chemically synthesized one. There are various methods reported in the literature for their synthesis, but most commonly used are physical, chemical, and biological methods. These biological methods are more eco-friendly and cost-effective [4].

Nanoparticles have different sizes and shapes within the diameter of 1–100 nm [5], hence termed as nanoparticles or nanomaterial. Numerous studies have focused on the potential applications of metallic nanoparticles, such as gold [6, 7], silver [8], platinum [9, 10], palladium [11, 12], and titanium [13, 14]. Bioavailability, behaviors, reactivity, stability, and toxicity of the nanoparticles [3, 15] are very important parameters to study the behavior of the nanoparticles.

Published online: 23 May 2019

Animals living in a specific ecosystem, when encountered with nanoparticles such as silver nanoparticles (AgNPs), their bodies respond to these materials adversely, but their toxicity levels and attributes vary from organism to organism or particles to particles. Silver nanoparticles (AgNPs) mainly induce the formation of reactive oxygen species (ROS), as major substances which induce oxidative stress, which further damage other cells and tissues of the organism [16, 17]. ROS include several oxygen–derived reactive molecules, such as hydroxyl radical (OH^{-1}), superoxide (O^{-2}), and hydrogen peroxide (H_2O_2). Production of ROS in a large amount may induce damages in biochemical pathways, as these radicals react with enzymes, nucleic acids, proteins, lipids of the biological membranes, and many other small molecules, which are very important to the biological system [18, 19] and metabolic pathways. Oxidative stress is primarily involved in the development of several acute and chronic diseases in human. Several studies have reported the effects of AgNPs in different organisms such as *Caenorhabditis elegans*, *Drosophila melanogaster*, and *Eisenia fetida* [16, 20, 21] in the invertebrates and vertebrate such as *Danio rerio* and *Mus musculus* [22, 23].

Ocimum tenuiflorum L. is synonymously termed as *Ocimum sanctum* L. and commonly termed as tulsi []. It is important medicinally, as it contains many active ingredients and effective against many diseases [25, 26]. It is an important plant with a long history in the sub-continent in drug therapy especially in Ayurvedic medicines, as it contains many active biomolecules; hence, we tried this plant as a capping and reducing agent for the synthesis of silver nanoparticles (AgNPs).

The aim of this study was to assess the acute toxicity associated with biologically and chemically synthesized AgNPs in the albino mice, and evaluate the safety profile of biologically synthesized AgNPs. To achieve this, we developed a study plan involving the synthesis and characterization of AgNPs, evaluation of LD-50, and determination of antioxidant enzymes activity in the liver and serum for both types of AgNPs after acute dosing.

2 Materials and Methods

Silver nitrate ($AgNO_3$) and other chemicals were purchased from Sigma-Aldrich. Deionized water was used in all experiments. The plant *Ocimum tenuiflorum* L. (tulsi) was obtained from the Botanical Garden Government College University, Lahore, Punjab, Pakistan.

2.1 Preparation of AgNPs (Biological Synthesis)

Biosynthesis of AgNPs was performed by the method [27] with slight modification. Ten grams of dried leaves of tulsi (*O. tenuiflorum*) were washed with distilled water carefully to remove extra dust particles and other impurities. Washed leaves were taken in 100 mL of deionized water and kept on the hot plate at 65 °C for 6–7 min with constant stirring, and plant extract was filtered using filter paper (Whatmann No.1). Silver nitrate ($AgNO_3$) (80 mL, 1 mM) and plant broth (20 mL) were poured in an Erlenmeyer flask and heated at 60 °C with magnetic stirring (200 RPM) for 8–10 min; the formation of nanoparticles was observed as the color changed to yellowish brown.

2.2 Preparation of AgNPs (Chemical Synthesis)

Silver nitrate (60 mL, 1 mM) was heated on the hot plate at 65 °C with constant stirring (200 RPM) for 6–7 min.

Trisodium citrate (6 mL, 10 mM) was added dropwise. After, a while solution color was changed to a light yellow, which indicated the formation of AgNPs [28].

2.3 Characterization of AgNPs

Characterization was performed by using general techniques, i.e., UV-visible spectrophotometry (GENESYS 10S UV-Vis), Fourier transform infra-red spectroscopy (FTIR) (Shimadzu IR Prestige21), and scanning electron microscopy (SEM) (JEOL, JSM-6480LV). Atomic absorption spectroscopy (AAS) was performed to observe the conversion of Ag ions into AgNPs (AA 7000F, Shimadzu, Japan). The concentration of the silver nanoparticles was analyzed by oven drying and lyophilization methods (ALPHA 1-4 LD).

2.4 Animals and Experimental Protocols

Albino mice (BALB/c) (10–12 weeks old with 28–40 g body weight) were obtained from animal house of the Government College University, Lahore, Pakistan. They were kept in cages provided with commercial rat pellets and regular water supplied with the help of ad libitum. They were housed in an air-conditioned room with a constant temperature range (22 ± 1 °C) and constant light/dark cycle (12:12 h). Acclimatization of the animals to the laboratory condition was achieved by keeping the animals in the cages for at least 7 days prior to dosing [29]. Animal care and handling were followed the official guidelines of OECD and was submitted by the Ethics Committee of the Government College University, Lahore, Pakistan.

2.5 Toxicity Studies (Evaluation of LD-50)

The acute toxicity was determined in mice through performing the lethal dose 50 (LD50) studies by using commercially adopted procedures [30] for both types of AgNPs. For this purpose, 2 batches of albino mice, each containing 8 groups with 10 mice in

each group, were kept in 8 cages. Eight concentrations of G. AgNPs (500, 600, 700, 800, 900, 1000, 1100, and 1200 mg/kg of the body weight) and C. AgNPs (200, 300, 400, 500, 600, 700, 800, and 900 mg/kg of the body weight) were prepared and administered via intravenous tail vein (IV administration). These doses were administered one concentration per group after every 24 h for 96 h (4 days). Hodge and Sterner's scale was used as a reference for toxicity [31]. Mortality of the mice was calculated after every 24 h. LD-50 was calculated by using the probit analysis method.

2.6 Acute Toxicity Studies

Sublethal doses, i.e., 100 mg/kg of the body weight of each type of AgNPs (i.v. administered), were used to evaluate the acute toxicity of the nanoparticles on mice. The experiment was performed in three batches, batch-I (7 days), batch-II (14 days), and batch-III (21 days). Each batch was divided into three groups: G1 (control; no AgNP exposure), G2 (100 mg/kg of G. AgNPs), and G3 (100 mg/kg of C. AgNPs), and each group contained 10 Mice. After the prerequisite period of treatment, mice were sacrificed, and blood and liver samples were obtained.

2.7 Serum Separation and Homogenate Formation

Blood samples were collected from the cardiac puncture in serum separator gel tubes, which were further centrifuged at 5000 rpm for 30 min. Serum samples were collected and stored at − 80 °C for future analysis. Livers were washed with buffer solution for a while, soaked in 9 mL of 0.1 M phosphate buffer (pH 7.4), and were homogenized in a Teflon tissue homogenizer. Homogenate was centrifuged for 10 min at the 12,000 rpm in a refrigerated centrifuge machine at 4 °C. The supernatant was collected and stored at − 20 °C for further analysis [32].

2.7.1 Estimation of Superoxide Dismutase

It was estimated as per the protocol of Marklund and Marklund [33]. Auto-oxidation of the pyrogallol is inhibited by the superoxide dismutase (SOD). Reaction chamber contained a final volume of 3.0 mL, containing 2.80 mL of (0.05 M) Tris-succinate buffer (pH 8.2), 100 μL of the sample. It was incubated at 25 °C for 20 min, 100 μL of 8 mM pyrogallol was added, and change in absorbance was measured at 412 nm with a time interval of the 30 s for 3 min. The specific activity is reported in units per milligram of protein or units per milliliter of the homogenate.

2.7.2 Estimation of Catalase

It was assayed according to the protocol described by Javed et al. [32]. A total volume of the reaction mixture was 3.0 mL, containing 1.90 mL of (50 mM) phosphate buffer (pH 7.0) and 100 μL of the sample material. One milliliter of hydrogen peroxide (H_2O_2) was added to initiate the reaction. The absorbance of the solution was measured at 240 nm for 3 min with an interval of 30 s.

2.7.3 Estimation of Glutathione-S-Transferase

Glutathione-S-transferase (GST) activity was analyzed using the method reported by Javed et al. [32]. The total volume of the reaction mixture was 1.5 ml, containing 1.35 mL of (0.1 M) phosphate buffer (pH 6.5), 50 μL of GSH, and 50 μL of the sample material. A 50 μL solution of 1-Chloro-2, 4-dinitrobenzene (CDNB) was added to initiate the reaction. The absorbance of the solution was measured at 340 nm for 5 min with a time interval of 30 s. Enzyme activity was expressed as units per milligram of protein.

3 Results and Discussion

3.1 Synthesis and Characterization of AgNPs

Ocimum tenuiflorum–synthesized nanoparticles were relatively stable for more than 6 weeks, which make them a good candidate for various applications. These results are in agreement with other similar studies previously reported; another study reported the stability of *O. tenuiflorum*–derived AgNPs for 2 months [34]. *Azadirachta indica*'s derived AgNPs were reported with high stability [35], and it is highly correlated with the pH of the medium. Plant extract–derived AgNPs have highly negative zeta potential, hence are stable in the wide range of pH [36]. Our results are totally in agreement with the previous reports [37–46].

3.2 Characterization of Silver Nanoparticles

3.2.1 UV-Visible Spectroscopy

We obtained UV peak at 425 nm for G. AgNPs and 416 nm for C. AgNPs, which indicate the formation of AgNPs with spherical shapes (Fig. 1a, b), smaller than 100 nm which could be used for further applications [47].

The surface plasmon resonance (SPR) band of the UV-visible has special peak ranging from 380 to 440 nm for spherical shaped AgNPs [48]. Due to the presence of surface plasmon resonance, vibrations, and excitation, AgNPs have a characteristic yellow color in suspension [49–51]. Similar results were reported for the *Ocimum sanctum*–mediated synthesis of AgNPs and peak at 406 nm was reported [52]. On the other hand, leaf extracts of *Eclipta prostrate* [53] and *Memecylon edule* [54] were reported to produce triangular, pentagonal, and hexagonal AgNPs. Shapes and sizes of the

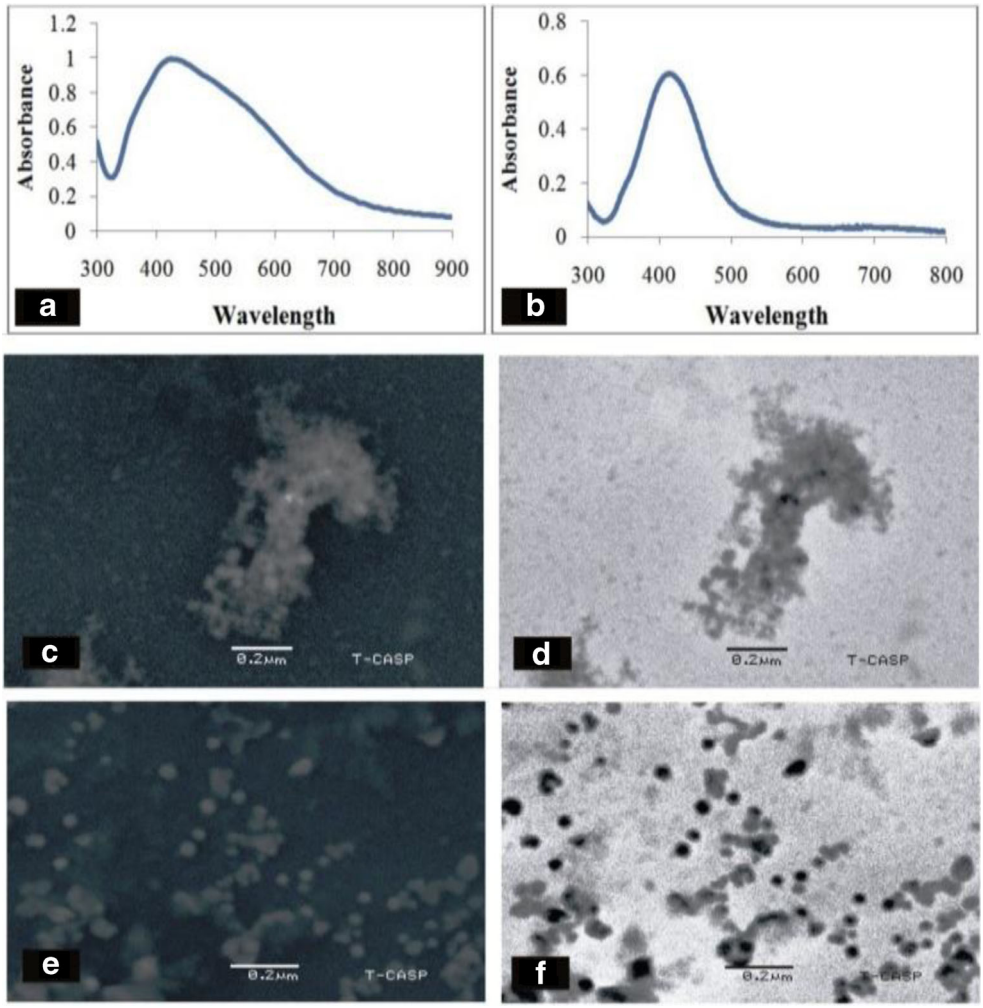

Fig. 1 UV-Vis spectrum of the **a** G. AgNPs, **b** C. AgNPs, **c** simple SEM of C. AgNPs, **d** inverted color SEM image of C. AgNPs, **e** simple SEM of G. AgNPs, and **f** inverted color SEM image of G. AgNPs

nanoparticles are mainly temperature and time dependent [55]. At 25 °C temperature, particles with large sizes (50 nm) were produced; however, at 95 °C, particle size was reduced to 16 nm [4]. Peak intensity increased with time, which indicated formation of more silver nanoparticles. Band peak variations are shape and size dependent, hence their peaks are obtained at variously specified region on the spectrum. Results obtained for UV-visible spectroscopy of the AgNPs synthesized are consistent with the previous studies [27, 38, 40, 46, 56, 57].

3.2.2 Scanning Electron Microscopy

The scanning electron microscopy (SEM) micrograph showed polydisperse, varied sized, and spherical shapes of the AgNPs. Size ranging from 40 to 60 nm for G. AgNPs (Fig. 1e, f), whereas from 30 to 40 nm for C. AgNPs (Fig. 1c, d). Similar results of the SEM were reported for AgNPs synthesized via using the extract of *Ocimum sanctum* [58]. Previous studies reported SEM analysis of *Piper longum*–derived spherical shaped AgNPs, with size ranging 17.6–41 nm [59], and spherical shaped AgNPs using *Alternanthera sessilis* with the size ranging from 20 to 30 nm [60]. On the other hand, green synthesis of AgNPs by using the leaf extract of *Eclipta prostrate* [53] and *Memecylon edule* [54] produced other shapes of nanoparticles, such as triangular, pentagonal, and hexagonal. Size of the nanoparticles depends upon the leaf broth concentration, concentration of $AgNO_3$, and temperature of the reaction [4]. The shape of the nanoparticles generally depends upon the nature of reducing and capping agent [40].

3.2.3 FTIR Analysis of Biosynthesized Silver Nanoparticles

Untreated extract of the *Ocimum tenuiflorum* leaf showed absorption bands at different wave numbers (cm^{-1}), i.e., 3311, 2931, 2881, 2376, 2349, 1614, 1404, 1298, 1060, 827, and 786 cm^{-1}.

When the FTIR spectra of the AgNPs were compared with the extract of the *O. tenuiflorum*, minute changes were observed in the position and magnitude of the absorption bands.

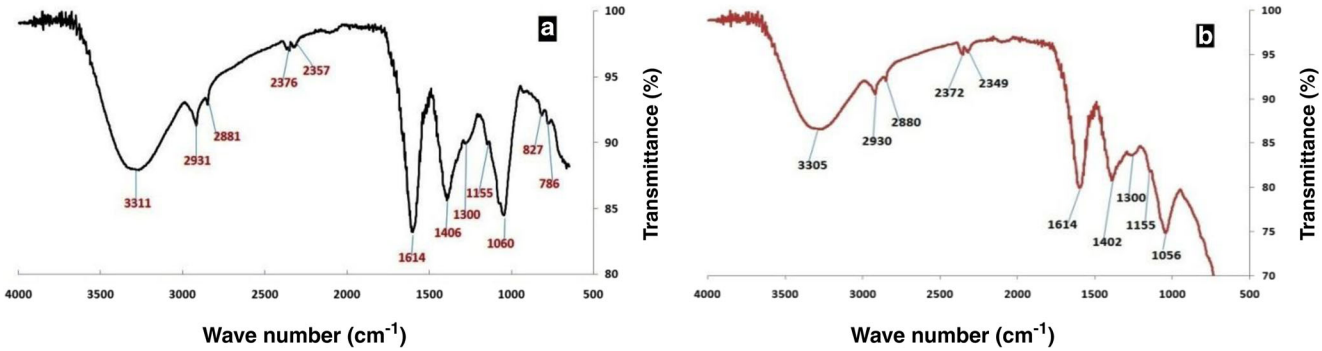

Fig. 2 FTIR Spectrum of **a** plant extract of *O. tenuiflorum* and **b** G. AgNPs

Variability in the wave number shift 1–10 cm^{-1} was observed, and the 2-min. band at 827 and 786 cm^{-1} disappeared in the spectra of the AgNPs prepared (Fig. 2). These bands indicated the aromatic stretching in the extract; hence, band disappearance indicated that the functional groups at these frequencies had taken part in the capping and reduction for the synthesis of AgNPs.

These results are in accordance with the previously studied FTIR analysis of the *Ocimum tenuiflorum* plant extract with slight variation in the peak of bands at certain positions [34]; also, it explained that the extract contained carboxylic, alcoholic, amine groups, and many other compounds. After the AgNP formation, slight changes in the magnitude and position were observed in the absorption bands of the spectrum. Few peaks were shortened and a few were diminished [34]. FTIR spectrum band at 3311 cm^{-1} is due to the stretching of O-H and H-bonded compounds such as phenols and alcohols. The absorption band at 2931 cm^{-1} indicated the presence of carboxylic acids due to the stretching of O-H. Bending of N-H of primary amine was attributed to the peak at 1614 cm^{-1}; other peaks correspond to the presence of the aromatic amine, ether, esters, ketones, and aldehydes groups present in the leaf extract of the *Ocimum* species [61]. Our results are in agreement with previous studies, as it indicated the consumption of alkenes and aromatic compounds as capping and the reducing agent. Other studies reported many other functional groups and biomolecules as capping and reducing agent: protein in *Capsicum annuum* [62]; theophylline and caffeine in tea [63]; phyllanthin in *Phyllanthus amarus* [64]; polyol, flavonoids, and terpenoids in *Cinnamomum camphora* leaf [65]; natural antioxidant [25, 66] in some other plant extract.

3.2.4 Atomic Absorption Spectroscopy

Total silver content after complete digestion of the silver nanoparticles was found to be 10.87 ± 0.91 μg/mL in G. AgNPs and 11.08 ± 0.26 μg/mL in C. AgNPs. Awwad [67] studied silver ions concentration in AgNPs with the help of atomic absorption spectroscopy (AAS), which further explained the conversion of the silver ions into nanoparticles, and time-dependent decrease in ions indicated the conversion of ions into AgNPs.

3.3 Toxicological Studies of AgNPs (Evaluation of LD 50)

The lethal dose (LD-50) was 812 mg/kg of the body weight (BW) for G. AgNPs and 575 mg/kg for C. AgNPs**.** Higher values for G. AgNPs make them less toxic and more eco-friendly. Previous reports described the LD-50 of the C. AgNPs in normal and irradiated mice as 268.781 mg/kg and 425.990 mg/kg of the body weight respectively [68]. Another study indicated the dose of LD-50 of the size-dependent AgNPs for albino mice was 169 and 213.8 mg/kg for 20 nm AgNPs and 354 and 391.5 mg/kg for 50 nm AgNPs; also, the particles with smaller size showed more toxicity as compared to the larger one [69]. Compared with other studies [68, 69], we prepared green synthesized silver nanoparticles (G. AgNPs) with higher values of LD-50 for G. AgNPs.

Table 1 Effects of silver nanoparticles on levels of superoxide dismutase (SOD) in mice liver tissues and serum, after administration of AgNPs through intravenous tail injections

SOD	7 days		14 days		21 days	
	Liver	Serum	Liver	Serum	Liver	Serum
Control	2.26 ± 0.27	4.24 ± 0.35	2.34 ± 0.45	4.50 ± 1.21	2.42 ± 0.46	4.33 ± 1.00
G. AgNPs	2.51 ± 0.39	4.75 ± 0.36	3.00 ± 0.77	5.01 ± 0.68	3.56 ± 0.81	4.94 ± 0.56
C. AgNPs	3.05 ± 0.99	5.98 ± 0.58	3.58 ± 0.92	5.31 ± 1.86	3.76 ± 0.95	5.17 ± 0.58

All the values are ±SEM of ($n = 10$)

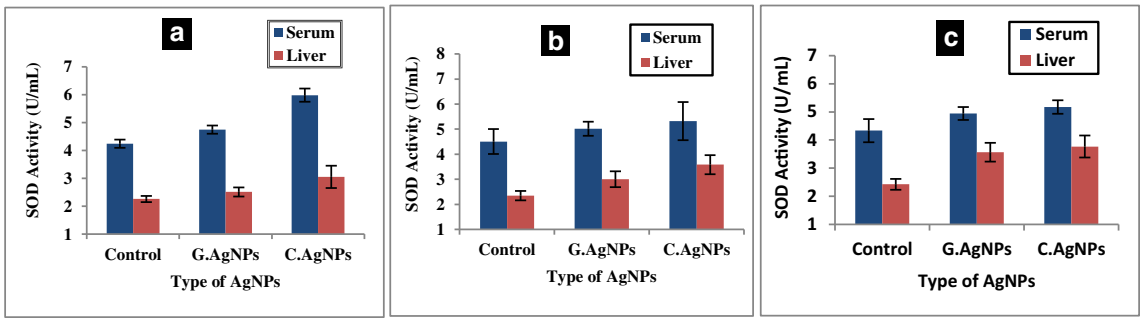

Fig. 3 Superoxide dismutase (SOD) activities with standard error mean in the liver tissue and serum samples after treatment of **a** 7 days, **b** 14 days, and **c** 21 days

Table 2 Effects of silver nanoparticles on levels of glutathione-S-transferase (GST) in mice liver tissues and serum, after administration

GST	7 days		14 days		21 days	
	Liver	Serum	Liver	Serum	Liver	Serum
Control	0.408 ± 0.01	0.411 ± 0.01	0.410 ± 0.01	0.414 ± 0.01	0.401 ± 0.01	0.412 ± 0.00
G. AgNPs	0.388 ± 0.02	0.367 ± 0.02	0.352 ± 0.02	0.339 ± 0.01	0.354 ± 0.02	0.350 ± 0.03
C. AgNPs	0.320 ± 0.01	0.355 ± 0.02	0.301 ± 0.01	0.304 ± 0.02	0.290 ± 0.01	0.281 ± 0.00

All the values are mean ± SEM ($n = 10$)

The plausible explanation for the higher value of LD-50 of G. AgNPs is relatively safer nature, as these nanoparticles are less toxic, hence showed higher LD-50 values compared to their counterpart. Generally, the smaller the LD-50 value, the more toxic the substance is and vice versa. Another possible explanation for this phenomenon is "size- and dose-dependent" biological activity of AgNPs in the body. Particles with the smaller sizes are more penetrating in the cell as compared to the larger particles.

3.4 Oxidative Stress and Liver Enzymology

The level of the superoxide dismutase (SOD) in both groups (G2 and G3) was increased as compared to the control group (G1) (Table 1). However, higher level of SOD was noticed in the G3 group as compared to the G2. Liver had lower value of SOD as compared to the serum; however, overall increasing trend was observed in both the values, i.e., serum and liver in all the batches of the mice (Fig. 3).

The level of the GST in both groups (G2 and G3) was increased as compared to the control group (G1) (Table 2). However, a higher level of the GST was recorded in the G3 group as compared to the G2. Liver contained slightly lower values of GST as compared to the serum; however, an overall decreasing trend was observed in both the values, i.e., serum and liver (Fig. 4) for all three batches.

The level of the catalase (CAT) in both groups (G2 and G3) was decreased as compared to the control group (G1) (Table 3). The however lower level of the CAT was noticed in the G3 group as compared to the G2. Liver contained slightly higher values of CAT as compared to the serum; however, an overall decreasing trend was observed in both the values, i.e., serum and liver (Fig. 5).

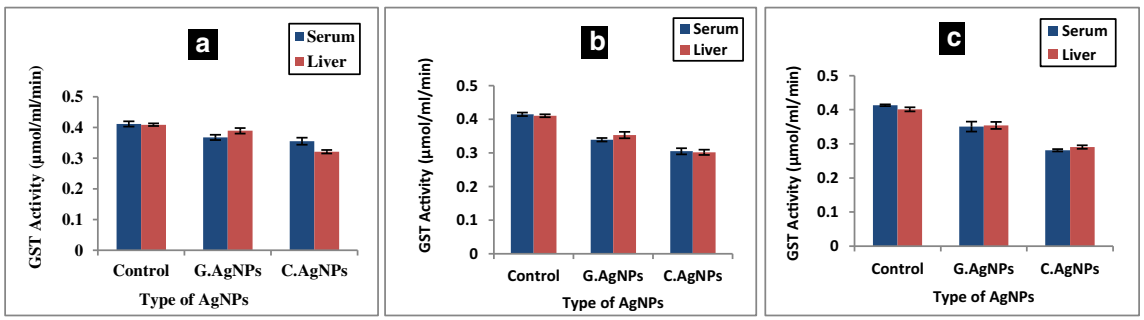

Fig. 4 Glutathione-S-transferase (GST) activities with standard error mean in the liver tissue and serum samples after treatment of **a** 7 days, **b** 14 days, and **c** 21 days

Table 3 Effects of silver nanoparticles on levels of catalase (CAT) in mice liver tissues and serum, after administration through intravenous tail injections

CAT	7 days		14 days		21 days	
	Liver	Serum	Liver	Serum	Liver	Serum
Control	86.00 ± 4.39	84.97 ± 2.54	86.23 ± 1.66	84.46 ± 3.19	86.69 ± 4.03	84.80 ± 1.03
G. AgNPs	82.68 ± 2.15	79.98 ± 2.59	78.89 ± 3.15	75.86 ± 2.27	81.30 ± 3.65	80.67 ± 0.34
C. AgNPs	72.82 ± 5.49	72.41 ± 2.47	69.15 ± 3.24	72.93 ± 6.90	76.72 ± 3.63	76.03 ± 2.66

All the values are ±SEM of ($n = 10$)

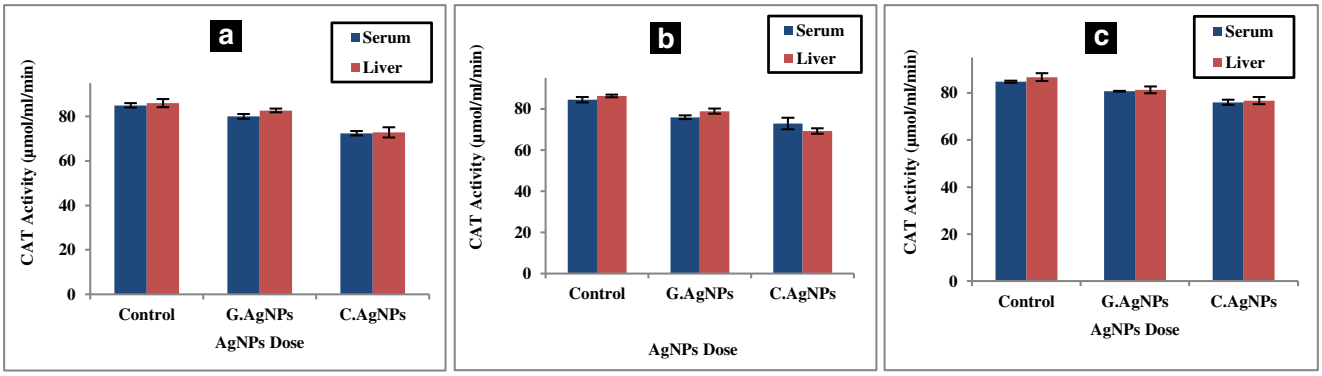

Fig. 5 Catalase (CAT) activities with standard error mean in the liver tissue and serum samples after treatment of **a** 7 days, **b** 14 days, and **c** 21 days

3.5 Oxidative Stress Under Sublethal Dose Effect

Groups of mice which were exposed to AgNPs showed a slight increase in the superoxide dismutase (SOD), while a decrease in the catalase (CAT) and glutathione-s-transferase (GST) activities (Fig. 6). Toxic effects of the nanoparticles for the biological systems need extensive investigations for better understanding. Various methods for toxicity evaluation have been developed, but proper indicators are still needed to be developed. Animal exposure to the AgNPs results in the formation of reactive oxygen species (ROS), the main source of oxidative stress, leading to disease development [70]. Tumor metastasis has been observed to cease, as ROS are removed by the antioxidant enzymes [71–73].

Other studies concerning oxidative stress for silver nanoparticles and other metallic nanoparticles reported a variety of results. Ashok et al. [74] reported that catalase, glutathione (GSH), and protein thiol significantly decreased, while the level of superoxide dismutase activity (SOD), lipid peroxidase, and glutathione peroxidase increased; our results are in agreement with this study. Another study reported increasing trends in the level of SOD [75]. Similar results were reported for Cd (cadmium) toxicity; rats showed significantly decreased activity level of antioxidant enzymes such as CAT,

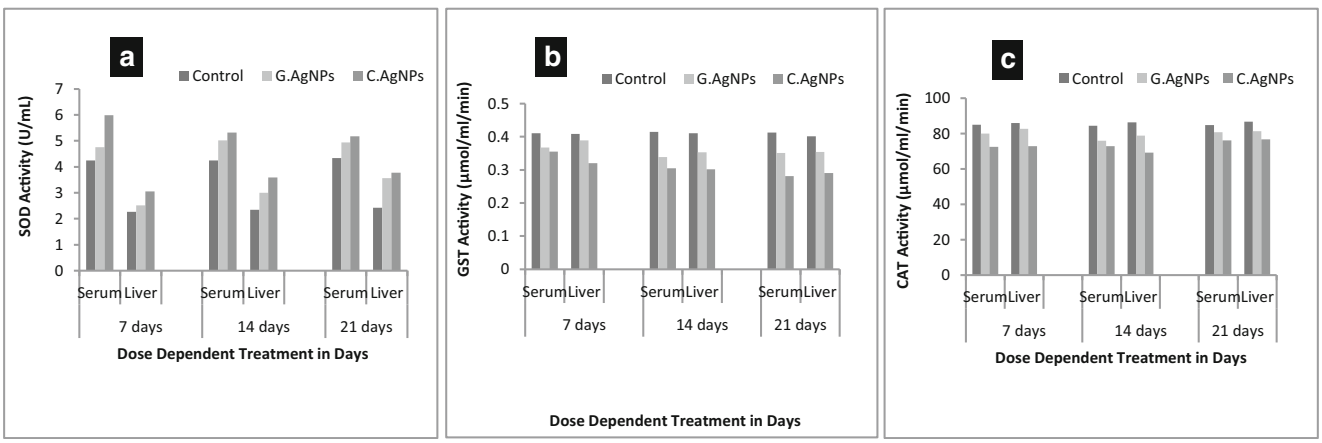

Fig. 6 Comparative analyses of serum and liver samples activity of **a** superoxide dismutase (SOD), **b** glutathione-S-transferase (GST), and **c** catalase (CAT)

GST, and SOD [76]. Disturbance in the level of these antioxidant enzymes clearly indicates the onset of oxidative stress in the animal body.

The plausible explanation for the phenomenon was given by Kim et al. [77]; animals were exposed to the AgNP-induced oxidative stress due to the mass generation of ROS, which significantly increased the antioxidant enzyme activity and resulted in a decreased level of free radicals [77]. More complications arise as antioxidant enzymes, glutathione (GSH), are depleted due to their over-consumption; intracellular calcium is increased [78] and it further activates other types of the cell signaling pathways using various calcium–dependent proteins in the cell cytosol.

Contrary to our result, an increase in the activity of CAT and glutathione peroxidase (GPx) was reported when animals were exposed to AgNPs; however, exposure to AuNPs and ZnO-NPs showed the opposite results with a significant decrease in values [79]. Another study on the hyperlipidemic rats [80] reported a significantly higher level of GST, CAT, and SOD upon exposure of uneaten pulp of the fruit from *Cordia dichotoma*. Studies on *medaka* liver reported a decreased level of the CAT and SOD in the liver cells; this could be explained by the fact that there was excessive utilization and consumption of these enzymes as the animal is in the oxidative stress [81]. However, there is need of further investigations for better insight and to resolve the matter of contradictory results in different studies.

AgNPs induced oxidative stress by various means in different animals [2, 17], but it needs more clarification at the molecular level. GPx, CAT, and SOD are the most important antioxidant enzymes which act as defense against naturally induced oxidative stress in the living systems [81]. Generally altered values of antioxidant enzymes from the normal indicate the acute toxicity of the AgNPs induced by oxidative stress, resulting in the enhanced production and activity of these enzymes [82]. This implies that C. AgNPs are more toxic than the G. AgNP, as oxidative stress when induced by a same dose of C.AgNPs (100 mg/kg of the body weight) is more severe.

The novelty of the work is to provide a comparative analysis of the oxidative stress caused by AgNP synthesis by two means, i.e., biological and chemical, and compare their risk assessment by evaluating the activity level of antioxidant enzymes in the liver and serum samples after exposure to the AgNPs for a specified period of time.

4 Conclusions

Synthesis of silver nanoparticles using plant, such as *Ocimum tenuiflorum*, is cost-effective as well as safer as compared to chemical synthesis method. Our studies involving AgNP–induced oxidative stress and their associated risk assessment in the albino mice show the induction of oxidative stress depending upon the physicochemical and oxidative properties of the nanoparticles, their interaction with the cellular machinery which in ROS generation. Our results suggest that green synthesized nanoparticles induce oxidative stress, but of mild nature as compared to enhanced toxicity of the chemically synthesized ones.

Recommendations Green synthesis route for the synthesis of AgNPs may be preferred instead of conventionally used chemical synthesis. Plant species other than *Ocimum* may be explored for their ability to yield safer nanoparticles. Studies may be initiated to understand whether green synthesized nanoparticles may have antibacterial or anticancerous properties compared to chemically synthesized one. Attempts may be done for better understanding of the same at cellular and molecular level. This opens new directions for scientists towards safer synthesis of nanoparticles and their extensive applications in biomedicals sciences with many other fields. We also suggest that environmental quality standards may be set for NPs for their safety profile in the light of the studies reported by far.

Acknowledgments The authors acknowledge Prof. Dr. Riaz Ahmad (Department of Physics) and Prof. Dr. Shazia Bashir (CASP), Government College University, Lahore, for providing facilities of characterization of nanoparticles.

Compliance with Ethical Standards

Animal care and handling were followed the official guidelines of OECD and was submitted by the Ethics Committee of the Government College University, Lahore, Pakistan.

Conflict of Interest The authors declare that they have no conflict of interest.

Research Involving Humans and Animals Statement None.

Informed Consent None.

Funding Statement None.

References

1. Handy, R. D., Owen, R., & Valsami-Jones, E. (2008). The ecotoxicology of nanoparticles and nanomaterials: current status, knowledge gaps, challenges, and future needs. *Ecotoxicology, 17*(5), 315–325.
2. Scown, T. M., Santos, E. M., Johnston, B. D., Gaiser, B., Baalousha, M., Mitov, S., Lead, J. R., Stone, V., Fernandes, T. F., & Jepson, M. (2010). Effects of aqueous exposure to silver nanoparticles of different sizes in rainbow trout. *Toxicological Sciences, 115*(2), 521–534.
3. Pettitt, M. E., & Lead, J. R. (2013). Minimum physicochemical characterization requirements for nanomaterial regulation. *Environment International, 52*, 41–50.

4. Song, J. Y., & Kim, B. S. (2009). Rapid biological synthesis of silver nanoparticles using plant leaf extracts. *Bioprocess and Biosystems Engineering, 32*(1), 79.
5. Kreyling, W. G., Semmler-Behnke, M., & Chaudhry, Q. (2010). A complementary definition of nanomaterial. *Nano Today, 5*(3), 165–168.
6. Skrabalak, S. E., Chen, J., Sun, Y., Lu, X., Au, L., Cobley, C. M., & Xia, Y. (2008). Gold nanocages: synthesis, properties, and applications. *Accounts of Chemical Research, 41*(12), 1587–1595.
7. Wyszogrodzka, G., Marszałek, B., Gil, B., & Dorożyński, P. (2016). Metal-organic frameworks: mechanisms of antibacterial action and potential applications. *Drug Discovery Today, 21*(6), 1009–1018.
8. Nair, L. S., & Laurencin, C. T. (2007). Silver nanoparticles: synthesis and therapeutic applications. *Journal of Biomedical Nanotechnology, 3*(4), 301–316.
9. Govindhan, M., Liu, Z., & Chen, A. (2016). Design and electrochemical study of platinum-based nanomaterials for sensitive detection of nitric oxide in biomedical applications. *Nanomaterials, 6*(11), 211.
10. Kanninen, P., Luong, N. D., Flórez-Montaño, J., Jiang, H., Pastor, E., Seppälä, J., & Kallio, T. (2017). Highly active platinum nanoparticles supported by nitrogen/sulfur functionalized graphene composite for ethanol electro-oxidation. *Electrochimica Acta, 242*, 315–326.
11. Xiong, Y., & Xia, Y. (2007). Shape-controlled synthesis of metal nanostructures: the case of palladium. *Advanced Materials, 19*(20), 3385–3391.
12. Karimi, R., Yousefi, F., Ghaedi, M., Dashtian, K., & Montazerozohori, M. (2017). Efficient adsorption of erythrosine and sunset yellow onto modified palladium nanoparticles with a 2-diamine compound: Application of multivariate technique. *Journal of Industrial and Engineering Chemistry, 48*, 43–55.
13. Coelho, S. G., Patri, A. K., Wokovich, A. M., McNeil, S. E., Howard, P. C., & Miller, S. A. (2016). Repetitive application of sunscreen containing titanium dioxide nanoparticles on human skin. *JAMA Dermatology, 152*(4), 470–472.
14. Mahmoud, W. M., Rastogi, T., & Kümmerer, K. (2017). Application of titanium dioxide nanoparticles as a photocatalyst for the removal of micropollutants such as pharmaceuticals from water. *Current Opinion in Green and Sustainable Chemistry, 6*, 1–10.
15. Tantra, R., Jing, S., Pichaimuthu, S. K., Walker, N., Noble, J., & Hackley, V. A. (2011). Dispersion stability of nanoparticles in ecotoxicological investigations: the need for adequate measurement tools. *Journal of Nanoparticle Research, 13*(9), 3765–3780.
16. Ahamed, M., Posgai, R., Gorey, T. J., Nielsen, M., Hussain, S. M., & Rowe, J. J. (2010). Silver nanoparticles induced heat shock protein 70, oxidative stress and apoptosis in Drosophila melanogaster. *Toxicology and Applied Pharmacology, 242*(3), 263–269.
17. Choi, J. E., Kim, S., Ahn, J. H., Youn, P., Kang, J. S., Park, K., Yi, J., & Ryu, D.-Y. (2010). Induction of oxidative stress and apoptosis by silver nanoparticles in the liver of adult zebrafish. *Aquatic Toxicology, 100*(2), 151–159.
18. Gülçin, İ., Oktay, M., Küfrevioğlu, Ö. İ., & Aslan, A. (2002). Determination of antioxidant activity of lichen Cetraria islandica (L) Ach. *Journal of Ethnopharmacology, 79*(3), 325–329.
19. Jayanthi, P., & Lalitha, P. (2011). Reducing power of the solvent extracts of Eichhornia crassipes (Mart.) Solms. *International Journal of Pharmacy and Pharmaceutical Sciences, 3*(3), 126–128.
20. Hayashi, Y., Heckmann, L.-H., Simonsen, V., & Scott-Fordsmand, J. J. (2013). Time-course profiling of molecular stress responses to silver nanoparticles in the earthworm Eisenia fetida. *Ecotoxicology and Environmental Safety, 98*, 219–226.
21. Ahn, J.-M., Eom, H.-J., Yang, X., Meyer, J. N., & Choi, J. (2014). Comparative toxicity of silver nanoparticles on oxidative stress and DNA damage in the nematode, Caenorhabditis elegans. *Chemosphere, 108*, 343–352.
22. Ghosh, M., Manivannan, J., Sinha, S., Chakraborty, A., Mallick, S. K., Bandyopadhyay, M., & Mukherjee, A. (2012). In vitro and in vivo genotoxicity of silver nanoparticles. *Mutation Research, Genetic Toxicology and Environmental Mutagenesis, 749*(1), 60–69.
23. Massarsky, A., Dupuis, L., Taylor, J., Eisa-Beygi, S., Strek, L., Trudeau, V. L., & Moon, T. W. (2013). Assessment of nanosilver toxicity during zebrafish (Danio rerio) development. *Chemosphere, 92*(1), 59–66.
24. Staples, G. Kristiansen MS (1999) Ethnic culinary herbs; a guide to identification and cultivation in Hawai'i/; George W. Staples, Michael S. Kristiansen.i. University of Hawaii Press.
25. Mondal, S., Mirdha, B. R., & Mahapatra, S. C. (2009). The science behind sacredness of Tulsi (Ocimum sanctum Linn.). *Indian Journal of Physiology and Pharmacology, 53*(4), 291–306.
26. Bindhani, B. K., & Panigrahi, A. K. (2015). Biosynthesis and characterization of silver nanoparticles (SNPs) by using leaf extracts of Ocimum Sanctum L (Tulsi) and study of its antibacterial activities. *Journal of Nanomedicine & Nanotechnology*, (S6), 1.
27. Singhal, G., Bhavesh, R., Kasariya, K., Sharma, A. R., & Singh, R. P. (2011). Biosynthesis of silver nanoparticles using Ocimum sanctum (Tulsi) leaf extract and screening its antimicrobial activity. *Journal of Nanoparticle Research, 13*(7), 2981–2988.
28. Turkevich, J., Stevenson, P. C., & Hillier, J. (1951). A study of the nucleation and growth processes in the synthesis of colloidal gold. *Discussions of the Faraday Society, 11*, 55–75.
29. Al Gurabi, M. A., Ali, D., Alkahtani, S., & Alarifi, S. (2015). In vivo DNA damaging and apoptotic potential of silver nanoparticles in Swiss albino mice. *OncoTargets and Therapy, 8*, 295.
30. Guideline, O. O. (2001). 425: acute oral toxicity—Up-and-down procedure. *OECD Guidelines for the Testing of Chemicals, 2*, 12–16.
31. Hodge A, Sterner B (2005) Toxicity classes in Canadian Centre for Occupational Health and Safety. Retrieved from http://www. ccohs. ca/oshanswers/chemicals/id50. htm.
32. Javed, M., Usmani, N., Ahmad, I., & Ahmad, M. (2015). Studies on the oxidative stress and gill histopathology in Channa punctatus of the canal receiving heavy metal-loaded effluent of Kasimpur Thermal Power Plant. *Environmental Monitoring and Assessment, 187*(1), 4179.
33. Marklund, S., & Marklund, G. (1974). Involvement of the superoxide anion radical in the autoxidation of pyrogallol and a convenient assay for superoxide dismutase. *European Journal of Biochemistry, 47*(3), 469–474.
34. Daniel, S., Kumar, R., Sathish, V., Sivakumar, M., Sunitha, S., & Sironmani, T. A. (2011). Green synthesis (Ocimum tenuiflorum) of silver nanoparticles and toxicity studies in zebra fish (Danio rerio) model. *International Journal of Nanoscience and Nanotechnology, 2*, 103–117.
35. Shankar, S. S., Rai, A., Ahmad, A., & Sastry, M. (2004). Rapid synthesis of Au, ag, and bimetallic Au core–Ag shell nanoparticles using Neem (Azadirachta indica) leaf broth. *Journal of Colloid and Interface Science, 275*(2), 496–502.
36. Mock, J., Barbic, M., Smith, D., Schultz, D., & Schultz, S. (2002). Shape effects in plasmon resonance of individual colloidal silver nanoparticles. *The Journal of Chemical Physics, 116*(15), 6755–6759.
37. Ahmad, N., Sharma, S., Alam, M. K., Singh, V., Shamsi, S., Mehta, B., & Fatma, A. (2010). Rapid synthesis of silver nanoparticles using dried medicinal plant of basil. *Colloids and Surfaces B: Biointerfaces, 81*(1), 81–86.
38. Awwad, A. M., Salem, N. M., & Abdeen, A. O. (2013). Green synthesis of silver nanoparticles using carob leaf extract and its

antibacterial activity. *International Journal of Industrial Chemistry, 4*(1), 29.

39. Borah, D., Deka, P., Bhattacharjee, P., Changmai, A., & Yadav, R. (2013). Ocimum sanctum mediated silver nanoparticles showed better antimicrobial activities compared to citrate stabilized silver nanoparticles against multidrug-resistant bacteria. *Journal of Pharmacy Research, 7*(6), 478–482.
40. Banerjee, P., Satapathy, M., Mukhopahayay, A., & Das, P. (2014). Leaf extract mediated green synthesis of silver nanoparticles from widely available Indian plants: synthesis, characterization, antimicrobial property and toxicity analysis. *Bioresources and Bioprocessing, 1*(1), 3.
41. Brahmachari, G., Sarkar, S., Ghosh, R., Barman, S., Mandal, N. C., Jash, S. K., Banerjee, B., & Roy, R. (2014). Sunlight-induced rapid and efficient biogenic synthesis of silver nanoparticles using aqueous leaf extract of Ocimum sanctum Linn. with enhanced antibacterial activity. *Organic and Medicinal Chemistry Letters, 4*(1), 18.
42. Malapermal, V., Botha, I., Krishna, S. B. N., & Mbatha, J. N. (2017). Enhancing antidiabetic and antimicrobial performance of Ocimum basilicum, and Ocimum sanctum (L.) using silver nanoparticles. *Saudi Journal of Biological Sciences, 24*(6), 1294–1305.
43. Ghaffari-Moghaddam, M., Hadi-Dabanlou, R., Khajeh, M., Rakhshanipour, M., & Shameli, K. (2014). Green synthesis of silver nanoparticles using plant extracts. *Korean Journal of Chemical Engineering, 31*(4), 548–557.
44. Sadanand, V., Rajini, N., Satyanarayana, B., & Rajulu, A. V. (2016). Preparation and properties of cellulose/silver nanoparticle composites within situ-generated silver nanoparticles using Ocimum sanctum leaf extract. *International Journal of Polymer Analysis and Characterization, 21*(5), 408–416.
45. Jha, P. K., Jha, R. K., Rout, D., Gnanasekar, S., Rana, S. V., & Hossain, M. (2017). Potential targetability of multi-walled carbon nanotube-loaded with silver nanoparticles photosynthesized from Ocimum tenuiflorum (tulsi extract) in fertility diagnosis. *Journal of Drug Targeting, 25*(7), 616–625.
46. Khan, M., Tarek, F., Nuzat, M., Momin, M., & Hasan, M. (2017). Rapid biological synthesis of silver nanoparticles from Ocimum sanctum and their characterization. *Journal of Nanoscience, 2017*.
47. Dehnavi, A. S., Aroujalian, A., Raisi, A., & Fazel, S. (2013). Preparation and characterization of polyethylene/silver nanocomposite films with antibacterial activity. *Journal of Applied Polymer Science, 127*(2), 1180–1190.
48. Stamplecoskie, K. G., & Scaiano, J. C. (2010). Light emitting diode irradiation can control the morphology and optical properties of silver nanoparticles. *Journal of the American Chemical Society, 132*(6), 1825–1827.
49. Mulvaney, P. (1996). Surface plasmon spectroscopy of nanosized metal particles. *Langmuir, 12*(3), 788–800.
50. Jensen, T. R., Malinsky, M. D., Haynes, C. L., & Van Duyne, R. P. (2000). Nanosphere lithography: tunable localized surface plasmon resonance spectra of silver nanoparticles. *The Journal of Physical Chemistry. B, 104*(45), 10549–10556.
51. Abdel-Aziz, M. S., Shaheen, M. S., El-Nekeety, A. A., & Abdel-Wahhab, M. A. (2014). Antioxidant and antibacterial activity of silver nanoparticles biosynthesized using Chenopodium murale leaf extract. *Journal of Saudi Chemical Society, 18*(4), 356–363.
52. Rao, Y. S., Kotakadi, V. S., Prasad, T., Reddy, A., & Gopal, D. S. (2013). Green synthesis and spectral characterization of silver nanoparticles from Lakshmi tulasi (Ocimum sanctum) leaf extract. *Spectrochimica Acta. Part A, Molecular and Biomolecular Spectroscopy, 103*, 156–159.
53. Rajakumar, G., & Rahuman, A. A. (2011). Larvicidal activity of synthesized silver nanoparticles using Eclipta prostrata leaf extract against filariasis and malaria vectors. *Acta Tropica, 118*(3), 196–203.
54. Elavazhagan, T., & Arunachalam, K. D. (2011). Memecylon edule leaf extract mediated green synthesis of silver and gold nanoparticles. *International Journal of Nanomedicine, 6*, 1265.
55. Song, J. Y., Kwon, E.-Y., & Kim, B. S. (2012). Antibacterial latex foams coated with biologically synthesized silver nanoparticles using Magnolia kobus leaf extract. *Korean Journal of Chemical Engineering, 29*(12), 1771–1775.
56. Vahabi, K., Mansoori, G. A., & Karimi, S. (2011). Biosynthesis of silver nanoparticles by fungus Trichoderma reesei (a route for large-scale production of AgNPs). *Insciences Journal, 1*(1), 65–79.
57. Vignesh, V., Anbarasi, K. F., Karthikeyeni, S., Sathiyanarayanan, G., Subramanian, P., & Thirumurugan, R. (2013). A superficial phyto-assisted synthesis of silver nanoparticles and their assessment on hematological and biochemical parameters in Labeo rohita (Hamilton, 1822). *Colloids and Surfaces A: Physicochemical and Engineering Aspects, 439*, 184–192.
58. Vijaya, P., Rekha, B., Mathew, A. T., Ali, M. S., Yogananth, N., Anuradha, V., & Parveen, P. K. (2014). Antigenotoxic effect of green-synthesised silver nanoparticles from Ocimum sanctum leaf extract against cyclophosphamide induced genotoxicity in human lymphocytes—in vitro. *Applied Nanoscience, 4*(4), 415–420.
59. Jacob, S. J. P., Finub, J., & Narayanan, A. (2012). Synthesis of silver nanoparticles using Piper longum leaf extracts and its cytotoxic activity against Hep-2 cell line. *Colloids and Surfaces B: Biointerfaces, 91*, 212–214.
60. Niraimathi, K., Sudha, V., Lavanya, R., & Brindha, P. (2013). Biosynthesis of silver nanoparticles using Alternanthera sessilis (Linn.) extract and their antimicrobial, antioxidant activities. *Colloids and Surfaces B: Biointerfaces, 102*, 288–291.
61. Mallikarjuna, K., Narasimha, G., Dillip, G., Praveen, B., Shreedhar, B., Lakshmi, C. S., Reddy, B., & Raju, B. D. P. (2011). Green synthesis of silver nanoparticles using Ocimum leaf extract and their characterization. *Digest Journal of Nanomaterials and Biostructures, 6*(1), 181–186.
62. Li, S., Shen, Y., Xie, A., Yu, X., Zhang, X., Yang, L., & Li, C. (2007). Rapid, room-temperature synthesis of amorphous selenium/protein composites using Capsicum annuum L extract. *Nanotechnology, 18*(40), 405101.
63. Krishnaraj, C., Jagan, E., Rajasekar, S., Selvakumar, P., Kalaichelvan, P., & Mohan, N. (2010). Synthesis of silver nanoparticles using Acalypha indica leaf extracts and its antibacterial activity against water borne pathogens. *Colloids and Surfaces B: Biointerfaces, 76*(1), 50–56.
64. Kasthuri, J., Kathiravan, K., & Rajendiran, N. (2009). Phyllanthin-assisted biosynthesis of silver and gold nanoparticles: a novel biological approach. *Journal of Nanoparticle Research, 11*(5), 1075–1085.
65. Huang, J., Li, Q., Sun, D., Lu, Y., Su, Y., Yang, X., Wang, H., Wang, Y., Shao, W., & He, N. (2007). Biosynthesis of silver and gold nanoparticles by novel sundried Cinnamomum camphora leaf. *Nanotechnology, 18*(10), 105104.
66. Zhou, Y., Lin, W., Huang, J., Wang, W., Gao, Y., Lin, L., Li, Q., Lin, L., & Du, M. (2010). Biosynthesis of gold nanoparticles by foliar broths: roles of biocompounds and other attributes of the extracts. *Nanoscale Research Letters, 5*(8), 1351.
67. Awwad, A. M., Salem, N. M., & Abdeen, A. O. (2012). Biosynthesis of silver nanoparticles using Olea europaea leaves extract and its antibacterial activity. *Nanoscience and Nanotechnology, 2*(6), 164–170.
68. Amin, Y. M., Hawas, A. M., El-Batal, A., & Elsayed, S. H. H. E. (2015). Evaluation of acute and subchronic toxicity of silver nanoparticles in normal and irradiated animals. *British Journal of Pharmacology and Toxicology, 6*(2), 22–38.
69. Elkhawass, E., Mohallal, M., & Soliman, M. (2015). Acute toxicity of different sizes of silver nanoparticles intraperitonally injected in

Balb/C mice using two toxicological methods. *International Journal of Pharmacy and Pharmaceutical Sciences, 7*(2), 94–99.
70. Lee, Y.-H., Cheng, F.-Y., Chiu, H.-W., Tsai, J.-C., Fang, C.-Y., Chen, C.-W., & Wang, Y.-J. (2014). Cytotoxicity, oxidative stress, apoptosis and the autophagic effects of silver nanoparticles in mouse embryonic fibroblasts. *Biomaterials, 35*(16), 4706–4715.
71. Monte, M., Davel, L., & de Lustig, E. S. (1997). Hydrogen peroxide is involved in lymphocyte activation mechanisms to induce angiogenesis. *European Journal of Cancer, 33*(4), 676–682.
72. Nonaka, Y., Iwagaki, H., Kimura, T., Fuchimoto, S., & Orita, K. (1993). Effect of reactive oxygen intermediates on the in vitro invasive capacity of tumor cells and liver metastasis in mice. *International Journal of Cancer, 54*(6), 983–986.
73. Yoshizaki, N., Mogi, Y., Muramatsu, H., Koike, K., Kogawa, K., & Niitsu, Y. (1994). Suppressive effect of recombinant human cu, Zn-superoxide dismutase on lung metastasis of murtne tumor cells. *International Journal of Cancer, 57*(2), 287–292.
74. Ashok, I., Sheeladevi, R., & Wankhar, D. (2015). Acute effect of aspartame-induced oxidative stress in Wistar albino rat brain. *Journal of Biomedical Research, 29*(5), 390.
75. Smitha, K., & Mukkadan, J. (2014). Effect of different forms of acute stress in the generation of reactive oxygen species in albino wistar rats. *Indian Journal of Physiology and Pharmacology, 58*(3), 228–231.
76. Jamakala, O., & Rani, U. A. (2015). Amelioration effect of zinc and iron supplementation on selected oxidative stress enzymes in liver and kidney of cadmium-treated male albino rat. *Toxicology International, 22*(1), 1.
77. Kim, S., Choi, J. E., Choi, J., Chung, K.-H., Park, K., Yi, J., & Ryu, D.-Y. (2009). Oxidative stress-dependent toxicity of silver nanoparticles in human hepatoma cells. *Toxicology In Vitro, 23*(6), 1076–1084.
78. Yin, N., Liu, Q., Liu, J., He, B., Cui, L., Li, Z., Yun, Z., Qu, G., Liu, S., & Zhou, Q. (2013). Silver nanoparticle exposure attenuates the viability of rat cerebellum granule cells through apoptosis coupled to oxidative stress. *Small, 9*(9–10), 1831–1841.
79. Negahdary, M., Chelongar, R., Zadeh, S. K., & Ajdary, M. (2015). The antioxidant effects of silver, gold, and zinc oxide nanoparticles on male mice in vivo condition. *Advanced Biomedical Research, 69*(4).
80. El-Newary, S. A., Sulieman, A., El-Attar, S., & Sitohy, M. (2016). Hypolipidemic and antioxidant activity of the aqueous extract from the uneaten pulp of the fruit from Cordia dichotoma in healthy and hyperlipidemic Wistar albino rats. *Journal of Natural Medicines, 70*(3), 539–553.
81. Wu, Y., & Zhou, Q. (2013). Silver nanoparticles cause oxidative damage and histological changes in medaka (Oryzias latipes) after 14 days of exposure. *Environmental Toxicology and Chemistry, 32*(1), 165–173.
82. Arya, E., Saha, S., Saraf, S. A., & Kaithwas, G. (2013). Effect of *Perilla frutescens* fixed oil on experimental esophagitis in albino Wistar rats. *BioMed Research International, 2013*.